







## Aerobic anoxygenic phototrophic bacteria correlate with picophytoplankton across the Atlantic Ocean but show unique vertical bioenergetics

Carlota R. Gazulla <sup>1,2,3\*</sup> Michal Koblížek <sup>4</sup> Jesús M. Mercado <sup>3</sup> Josep M. Gasol <sup>2</sup> Olga Sánchez <sup>1</sup>  
Isabel Ferrera <sup>3\*</sup>

<sup>1</sup>Departament de Genètica i Microbiologia, Universitat Autònoma de Barcelona, Bellaterra, Barcelona, Spain

<sup>2</sup>Departament de Biologia Marina i Oceanografia, Institut de Ciències del Mar, ICM-CSIC, Barcelona, Catalunya, Spain

<sup>3</sup>Centro Oceanográfico de Málaga, Instituto Español de Oceanografía, IEO-CSIC, Málaga, Spain

<sup>4</sup>Laboratory of Anoxygenic Phototrophs, Institute of Microbiology of the Czech Academy of Sciences, Třeboň, Czechia

### Abstract

Aerobic anoxygenic phototrophic (AAP) bacteria are a common part of microbial communities in the sunlit ocean. They contain bacteriochlorophyll *a* (BChl *a*)-based photosystems that harvest solar energy for their metabolism. Across different oceanic regions, AAP bacteria seem to be more abundant in eutrophic areas, associated with high chlorophyll concentrations. While most previous studies focused on surface samplings, there is limited information regarding their vertical distribution in euphotic zones of the major ocean basins. Here, we hypothesized that AAP bacteria will follow a similar structure to the chlorophyll depth profile across areas with different degrees of stratification. To test this hypothesis, we enumerated AAP cells and determined bulk water BChl *a* concentrations along the photic zone of a latitudinal transect in the South and Central Atlantic Ocean. Overall, the distribution of AAP bacteria was highly correlated to that of chlorophyll *a* and to the abundance of picophytoplankton across both vertical and horizontal gradients. Furthermore, estimated light energy captured across the water column showed that, while AAP bacteria share a common latitudinal pattern of light absorption with picophytoplankton, they display a unique vertical arrangement with highest photoheterotrophic activity in the top 50 m of the surface ocean.

The epipelagic zone, where there is enough light to sustain primary production, hosts a vast array of microorganisms that drive biogeochemical transformations and sustain life in the global ocean. Within the surface ocean, replete with oxygen and lacking reduced nutrients, the phytoplankton and other primary producers provide a continuous supply of dissolved organic matter that supports the growth of heterotrophic bacteria, which in turn incorporate carbon into the base of the microbial food web (Azam et al. 1983). Besides the purely

autotrophic and heterotrophic organisms, there are a number of photoheterotrophic species which harvest light energy, but require organic matter for growth. Alongside proteorhodopsin (PR)-containing bacteria (Béjà et al. 2000), aerobic anoxygenic phototrophic (AAP) bacteria have garnered the attention of microbial ecologists since their discovery as common members of the surface ocean (Kolber et al. 2000). Aerobic anoxygenic phototrophic bacteria usually represent 1–7% of total bacteria in the euphotic zone (Koblížek 2015), they have large sizes compared to other bacteria (Sieracki et al. 2006), and higher growth rates (Koblížek et al. 2007; Ferrera et al. 2011; Fecskeová et al. 2021; Koblížek et al. 2024). Besides, they are subjected to a high grazing pressure (Ferrera et al. 2011; Koblížek et al. 2024), and as a result, their contribution to secondary production is more significant than their abundances alone would predict. This makes AAP bacteria dynamic members of the marine microbial life and important components of the carbon cycle in the ocean.

Aerobic anoxygenic phototrophic bacteria harvest light using photosystems containing bacteriochlorophyll *a* (BChl *a*). In contrast to their close relatives, the purple nonsulfur

\*Correspondence: lotaruiz@gmail.com; isabel.ferrera@ieo.csic.es

Additional Supporting Information may be found in the online version of this article.

This is an open access article under the terms of the [Creative Commons Attribution](https://creativecommons.org/licenses/by/4.0/) License, which permits use, distribution and reproduction in any medium, provided the original work is properly cited.

**Author Contribution Statement:** CRG and IF conceived the study. IF, JMM, OS, and JMG acquired funding. IF collected the samples. MK and CRG analyzed the samples. CRG processed the data and wrote the first draft. All authors contributed significantly to interpretation of results and reviewed the manuscript.

bacteria, they are strict aerobes and inhabit oxic environments (Madigan and Jung 2009; Imhoff 2017). Upon their discovery, it was speculated that AAP bacteria would be more prevalent in oligotrophic ocean regions (Kolber et al. 2000). However, subsequent studies showed that AAP bacteria are actually more abundant in productive regions or shelf seas (Mašín et al. 2006; Ritchie and Johnson 2012; Vrdoljak et al. 2019), coastal lagoons (Lamy et al. 2011), and estuaries (Schwalbach and Fuhrman 2005; Cottrell et al. 2010), where they can account for up to 12% of the total prokaryotic community. Nevertheless, in oligotrophic sites such as the Sargasso Sea or the North Pacific gyre, their relative contribution to total bacterial abundance is lower than 2% (Cottrell et al. 2006; Sieracki et al. 2006; Jiao et al. 2007; Koblížek et al. 2024). While AAP bacteria are common throughout the entire epipelagic zone, and they have even been isolated from the bathypelagic ocean (Rathgeber et al. 2008), most studies have focused on surface samples. The few studies that have dealt with their vertical distribution in the ocean showed that AAP bacteria had different abundance trends to those observed for heterotrophic bacteria or cyanobacteria (Cottrell et al. 2006; Sieracki et al. 2006; Jiao et al. 2007; Lami et al. 2007). Across the Mediterranean Sea, higher AAP abundance (Hojerová et al. 2011) and BChl *a* concentrations (Gómez-Consarnau et al. 2019) were observed above or overlapping the deep chlorophyll maximum (DCM). Altogether, these results suggest that AAP bacteria could be associated with phytoplankton not only in the ocean surface, but also along the water column.

Additionally, and in contrast to the growing knowledge on the distribution of AAP bacteria, there is little information regarding their phototrophic activity (i.e., light capture) in the natural environment. Laboratory studies with AAP culture isolates showed that light exposure reduced their respiration rate (Harashima et al. 1982; Koblížek et al. 2010; Hauruseu and Koblížek 2012), and increased the efficiency of carbon metabolism (Piwoż et al. 2018). As a result, cultures grown on light and dark regime accumulated more biomass than those kept in the dark (Yurkov and van Gemerden 1993; Biebl and Wagner-Döbler 2006; Hauruseu and Koblížek 2012; Piwoż et al. 2018). Light stimulation of growth on natural AAP bacterial populations was also demonstrated in field experiments (Ferrera et al. 2017; Sánchez et al. 2017, 2020). In addition, theoretical estimates indicate that AAP bacteria harvest more light energy per cell than PR-containing bacteria (Kirchman and Hanson 2013). However, estimates of actual light energy fluxes in the marine environment are scarce. By determining AAP abundance and pigment concentration we can calculate the light energy captured by AAP cells, providing information on their in situ physiology and, ultimately, allowing estimation of their potential phototrophic activity.

Here, we studied in detail the distribution of AAP bacteria along the water column in areas of contrasting productivity across the South and Central Atlantic Ocean. We took samples in 27 stations at different depths following the fluorescence

variation depicted by the CTD (conductivity, temperature, depth) profiler and enumerated AAP bacteria in addition to other photosynthetic microorganisms. We hypothesized that the distribution of AAP bacteria along the water column would be strongly connected to the DCM structure, with higher abundances in more productive sites. In addition, we used an improved high-performance liquid chromatography (HPLC) protocol to accurately detect picomolar (pM) concentrations of BChl *a* in the water column. Based on the microscopic and pigment data, we estimated the light energy captured by both BChl *a* and chlorophyll *a* (Chl *a*), and described how they varied spatially and along the depth gradient.

## Materials and methods

### Sampling

The POSEIDON Expedition took place between March and April 2019, on board the Spanish *RV Sarmiento de Gamboa*. It covered a distance of ~ 9000 km across a latitudinal transect (48°S/26°N) in the Atlantic Ocean. A total of 27 stations were sampled at different depths along the epipelagic zone. Seawater was collected using Niskin bottles mounted on a rosette equipped with a SeaBird 911-plus CTD. The CTD profiler was used to determine the depth variation of temperature, salinity, conductivity, fluorescence, turbidity, and dissolved oxygen. The fluorescence values from the CTD allowed to define the DCM structure along the water column for each station and, according to this structure, we took samples at the surface (fixed at 5 m deep), the DCM (depth at which the chlorophyll was maximal), the shallowest depth where chlorophyll fluorescence was undetectable (below the DCM), and then at different points where fluorescence increased (above the DCM) or decreased (below the DCM). Six of these stations were sampled at a higher resolution (10 sampled depths across the DCM structure). In two stations, the DCM structure displayed two peaks of chlorophyll maxima and samples were taken in each peak as well as between peaks (stations 10 and 16). The concentration of inorganic nutrients, specifically nitrate, nitrite, phosphate, and silicate were determined following the procedures outlined in González-Vega et al. (2023). Stations were numbered from 1 to 28, yet there were no samples from station 15 in our dataset. In total, 172 samples were collected from different depths ranging from 5 to 280 m. All seawater samples were prefiltered by a 200- $\mu$ m mesh to remove large plankton.

### Cell abundances

Samples (1.6 mL) were fixed using a solution of 1% paraformaldehyde + 0.05% glutaraldehyde (final concentrations), deep frozen in liquid nitrogen and stored at -80°C until analyzed. Heterotrophic prokaryotes, cyanobacteria, and photosynthetic picoeukaryotes abundances were determined by flow cytometry as described in Gasol and Morán (2015). Additionally, heterotrophic bacteria (i.e., prokaryotes),

cyanobacteria, and AAP bacteria were counted using infrared epifluorescence microscopy (Mašín et al. 2006) with recent modifications (Piwosz et al. 2022). Nine milliliters of seawater were fixed with formaldehyde to a final concentration of 3.7% and filtered onto white 25-mm polycarbonate filters of 0.2  $\mu\text{m}$  pore size (Nuclepore; Whatman). Cells were stained with 4'6-diamidino-2-phenylindole (DAPI) and counted using an epifluorescence Zeiss Axio Imager.D2 microscope equipped with a Plan-Apochromat 63 $\times$ /1.46 Oil Corr objective and a Collibri LED module illumination system (Carl Zeiss). Images for DAPI fluorescence (total bacteria) were taken under blue emission, the autofluorescence of Chl *a* was recorded in the red part of the spectrum and both BChl *a* and Chl *a*-containing bacteria were recorded in the infrared part of the spectrum. To obtain net BChl *a*-containing bacterial counts, the contribution of Chl *a*-containing organisms to the infrared image was subtracted as in Cottrell et al. (2006). We took at least 10 microphotographs for every sample and analyzed them with the ACMEtool2.0 software (Bennke et al. 2016). Based on the dissolved oxygen concentration (mean  $4.37 \pm 0.92 \text{ mg L}^{-1}$ ; Supporting Information Fig. S1), previous molecular studies from the same area (Gazulla et al. 2022), and preliminary molecular analyses of the *pufM* gene in the same transect (Gazulla 2024), we can safely assume that all BChl *a*-containing cells in our samples corresponded to AAP bacteria and not to any other type of anoxygenic phototrophs.

### Pigment analyses

Pigment composition in seawater samples was analyzed using an improved high-performance liquid chromatography (HPLC) protocol derived from the method of Goericke and Repeta (1993). Between 1 and 2 liters of seawater were prefiltered through a 200- $\mu\text{m}$  mesh, and then collected onto 25-mm polyethersulfone (PES) 0.45- $\mu\text{m}$ -pore size filter discs (Meck Millipore Ltd.) to assure that most AAP cells were captured (Lami et al. 2009). The use of 25-mm PES filters also reduced the required volume of filtered seawater and extraction solvents needed, and simplified the extraction protocol. Filters were conserved at  $-80^\circ\text{C}$  until pigment extraction which was conducted in the laboratory. Each filter was transferred to a cryogenic vial with 1 mL of 7:2 acetone:methanol (v/v) mixture and  $\sim 30 \text{ mg}$  of glass beads, and then disintegrated in a Mini-Beadbeater<sup>TM</sup> (Biospec Products) during 2 min, to break it and extract the pigments. After a short centrifugation (3 min, 14,100 rcf), the extracts were transferred to HPLC vials for further processing. We used a SCL-40 HPLC (Nexera series) equipped with SPD-M40 PDA detector and a UV-VIS detector with a deuterium (D2) lamp. For each sample, 50  $\mu\text{L}$  was injected into the system. Pigments were separated using a heated ( $40^\circ\text{C}$ ) Kinetex<sup>®</sup> 2.6  $\mu\text{m}$  C8 100 Å column (Phenomenex Inc.) with binary solvent system consisting of A: 75% methanol + 25% 28 mM ammonium acetate, and B: 100% methanol, with a flow rate of  $1 \text{ mL min}^{-1}$ . The gradient was the following: A/B 100/0 (0 min), A/B 0/100 (21 min), 0/100 (23 min), 100/0 (24 min), and 100/0 (25 min).

The peak for BChl *a* was registered at 770 nm. The pigment concentration in the original samples was calculated from the peak area. The use of Kinetex<sup>®</sup> column with core shell technology resulted in sharper peaks, which helped to accurately integrate small BChl *a* peaks. The peak of Chl *a* and divinyl-chlorophyll *a* was integrated together at 656 nm, so values of Chl *a* presented in the results included both Chl *a* and divinyl-chlorophyll *a*. The HPLC system was calibrated using 100% methanol extracts of *Synechocystis* sp. PCC6803 for Chl *a* and *Rhodobacter sphaeroides* for BChl *a*, where the concentrations of Chl *a* and BChl *a* were determined spectroscopically using a Shimadzu UV2600 spectrometer. From the BChl *a* concentration and AAP cell abundances, the BChl *a* cell quota was calculated as the quantity of BChl *a* per cell.

### Satellite-derived variables and irradiance per depth calculations

Given that no in situ photosynthetic active radiation (PAR) data could be measured during the cruise, satellite-derived PAR and diffuse attenuation coefficients at 490 nm ( $K_d$ ) were obtained from the Suomi-NPP/Visible Infrared Imaging Radiometer Suite instrument (SNPP-VIIRS). Eight-day composites at 9.28 km resolution (level 3-mapped data) were downloaded from the NASA Ocean Color Web (<https://oceancolor.gsfc.nasa.gov/l3/>). Both variables for each station were extracted according to the sampling date and the station coordinates. In case of data gaps due to clouds, the average values of a  $10 \times 10$  pixel square centered on the station coordinates were calculated. In situ irradiance per depth ( $\text{PAR}_{(z)}$ ) was calculated as:

$$\text{PAR}_{(z)} = \text{PAR}_{(0)} e^{-(K_d)z} \quad (1)$$

where  $\text{PAR}_{(0)}$  is the subsurface average daily downward irradiance for each station, assuming an average surface reflectance of 6%,  $z$  is the depth in meters, and  $K_d$  is the diffuse attenuation coefficient determined for each station. In Eqs. 2 and 3,  $\text{PAR}_{(z)}$  is denoted as  $I$  (irradiance).

### Bioenergetic calculations

The cellular daily energy captured per each cell was estimated applying the theoretical calculations of Kirchman and Hanson (2013) for AAP bacteria, assuming a hyperbolic response to light, as in Gómez-Consarnau et al. (2019). First, the number of photosynthetic units (PSU) per cell was calculated, considering that AAP bacteria contain a constant number of 34 molecules of BChl *a* per PSU (Yurkov and Beatty 1998; Koblížek et al. 2010), and assuming an average number of 300 molecules of Chl *a* per PSU in the case of the autotrophic picoplankton as in Gómez-Consarnau et al. (2019). AAP abundances were obtained through microscopic analyses, and the abundances of the autotrophic picoplankton were estimated as the sum of the abundances of *Prochlorococcus*, *Synechococcus*, and picoeukaryotes from the flow cytometry analyses. These calculations were applied to stations 5 to 28,

and we decided to remove stations 1 to 4 from the analysis, since we observed that a large fraction of the phytoplankton in samples from these stations was diatoms and could alter our estimations (i.e., picophytoplankton was a smaller fraction of total phytoplankton in those stations). As suggested by Kirchman and Hanson (2013), we considered that electron fluxes vary with irradiance in a Michaelis–Menten type relationship as:

$$V = \frac{V_{\max} \times I}{K_m + I} \quad (2)$$

where  $V_{\max}$  is the maximum flux and  $K_m$  is the half saturation constant, that is, the value of irradiance ( $I$ ) at which  $V$  is half of  $V_{\max}$ . The values of  $V_{\max}$  and  $K_m$  used in the equations as well as the energy per photon ( $E_0$ ) for BChl  $a$  and Chl  $a$  were extracted from Kirchman and Hanson (2013).

$$\text{Cellular daily energy yield (J cell}^{-1} \text{d}^{-1}) = \frac{\text{PSU}}{\text{cell}} \times V \times E_0 \times \frac{1}{T} \quad (3)$$

The cellular daily energy yield was estimated as in Eq. 3, where  $E_0$  is the energy per photon and  $T$  is the daylight seconds at each station. The day length at each site was calculated considering the sampling date, latitude, and longitude, with the NOAA Sunrise/Sunset Calculator (<https://gml.noaa.gov/grad/solcalc/sunrise.html>). The day length varied between 12.12 h (43,620 s) and 13.25 h (47,700 s).

### Statistics and data representation

Ocean Data View v5.6.5 was used to represent sectional distribution images. All calculations, data processing, and the rest of figures were performed in the R Core v4.3.3 environment (R Core Team 2024), using *tidyverse* (Wickham et al. 2019) and *ggplot2* (Wickham 2016). Correlation analyses to compare AAP bacteria abundances and BChl  $a$  concentrations with biotic and abiotic variables were performed using the *rcorr* function from the *Hmisc* package (Harrell 2024). The  $p$ -values were adjusted using Bonferroni corrections. For the PSU concentration values and light energy captured at the different DCM layers, we applied analyses of variance using the *aov* function and the post hoc Tukey's "Honest Significant Difference" method with function *TukeyHSD* from the *Stats* v4.3.3 package.

## Results

### Oceanographic context

The transect went from south to north starting in a region of high productivity in the South Atlantic characterized by low temperatures (mean 9.28°C) and relatively low salinity values (mean 34.18), influenced by their proximity to the Southern Ocean (stations 1 and 2, beyond 40°S; Supporting Information Fig. S1). Chlorophyll  $a$  and nutrient concentrations were high in these southernmost stations, especially silicate (mean

5.53  $\mu\text{M}$  in this area vs. 2.15  $\mu\text{M}$  in the whole transect). Noteworthy, the HPLC analyses of samples from these stations indicated high values of fucoxanthin (details not shown), the characteristic pigment of diatoms. In subsequent stations toward the north, temperature and salinity increased up to the maximal values recorded in the transect (temperature > 28.50°C and salinity > 37) in stations 10–14. These stations, located within the South Atlantic oligotrophic gyre (Fig. 1), had very low values of surface Chl  $a$ , and the DCMs (deep chlorophyll maxima) appeared below 120 m depths (Fig. 2a). In addition, light reached down to 200 m, while in the rest of the dataset, it did not surpass 100 m of depth (Supporting Information Fig. S1). The lowest values of nitrite, nitrate, phosphate, and silicate were recorded in the oligotrophic gyre (Supporting Information Fig. S2). In this area, two stations displayed a two-peak DCM structure (stations 10 and 16), with the shallowest peak located at ~50 and ~25 m depth, respectively. The deeper DCM peaks, at depths of ~100 and ~80 m, had the highest Chl  $a$  concentrations (Fig. 2a). As the cruise progressed toward the equator, the DCMs were shallower (between 50 and 100 m deep) and characterized by higher values of Chl  $a$  and nutrient concentrations. Finally, beyond the equator, seawater temperatures remained at around 20°C, but salinity increased as we were approaching the North-Atlantic oligotrophic gyre. Stations 23–28 had low nutrient levels and strong vertical mixing due to the upwelling waters off the coast of Mauritania. Along the transect, the fluorescence values obtained with the CTD probe were highly correlated with the Chl  $a$  concentration estimated by HPLC analyses ( $n = 146$ , Pearson correlation  $R = 0.90$ ,  $p < 0.0001$ ; Supporting Information Fig. S3), indicating that the profiling of the DCM structure on board was accurate.

### Bacterioplankton abundance variation across a vertical and horizontal gradient

Bacterioplankton (i.e., bacteria and archaea) concentrations varied between  $5.83 \times 10^4$  and  $1.28 \times 10^6$  cells  $\text{mL}^{-1}$  (mean  $\pm$  standard deviation [SD],  $3.58 \times 10^5 \pm 2.39 \times 10^5$  cells  $\text{mL}^{-1}$ ) and were mostly concentrated between 0 and 75 m depth, with a very similar distribution of high nucleic acid-containing (HNA) and low nucleic acid-containing (LNA) prokaryotes in all samples (Supporting Information Fig. S4). A high proportion of the bacterioplankton cells were *Prochlorococcus* (mean  $\pm$  SD, 44.75%  $\pm$  3.33%), which dominated in almost all stations and depths with values between  $10^5$  and  $10^6$  cells  $\text{mL}^{-1}$ . *Synechococcus* oscillated between  $10^2$  and  $10^4$  cells  $\text{mL}^{-1}$  and their abundance increased toward the boundary areas of the oligotrophic gyre (Supporting Information Fig. S4). Plastidic picoeukaryotes were more abundant at the DCM, in eutrophic areas, with densities up to  $10^4$  cells  $\text{mL}^{-1}$  (mean  $\pm$  SD,  $1.58 \times 10^3 \pm 2.65 \times 10^3$  cells  $\text{mL}^{-1}$ ). Altogether, autotrophic picoplankton—*Synechococcus*, *Prochlorococcus*, and picoeukaryotes—ranged between  $5.91 \times 10^4$  and  $1.16 \times 10^6$  cells  $\text{mL}^{-1}$  (mean  $\pm$  SD,  $3.05 \times 10^5 \pm 2.04 \times 10^5$  cells  $\text{mL}^{-1}$ ;



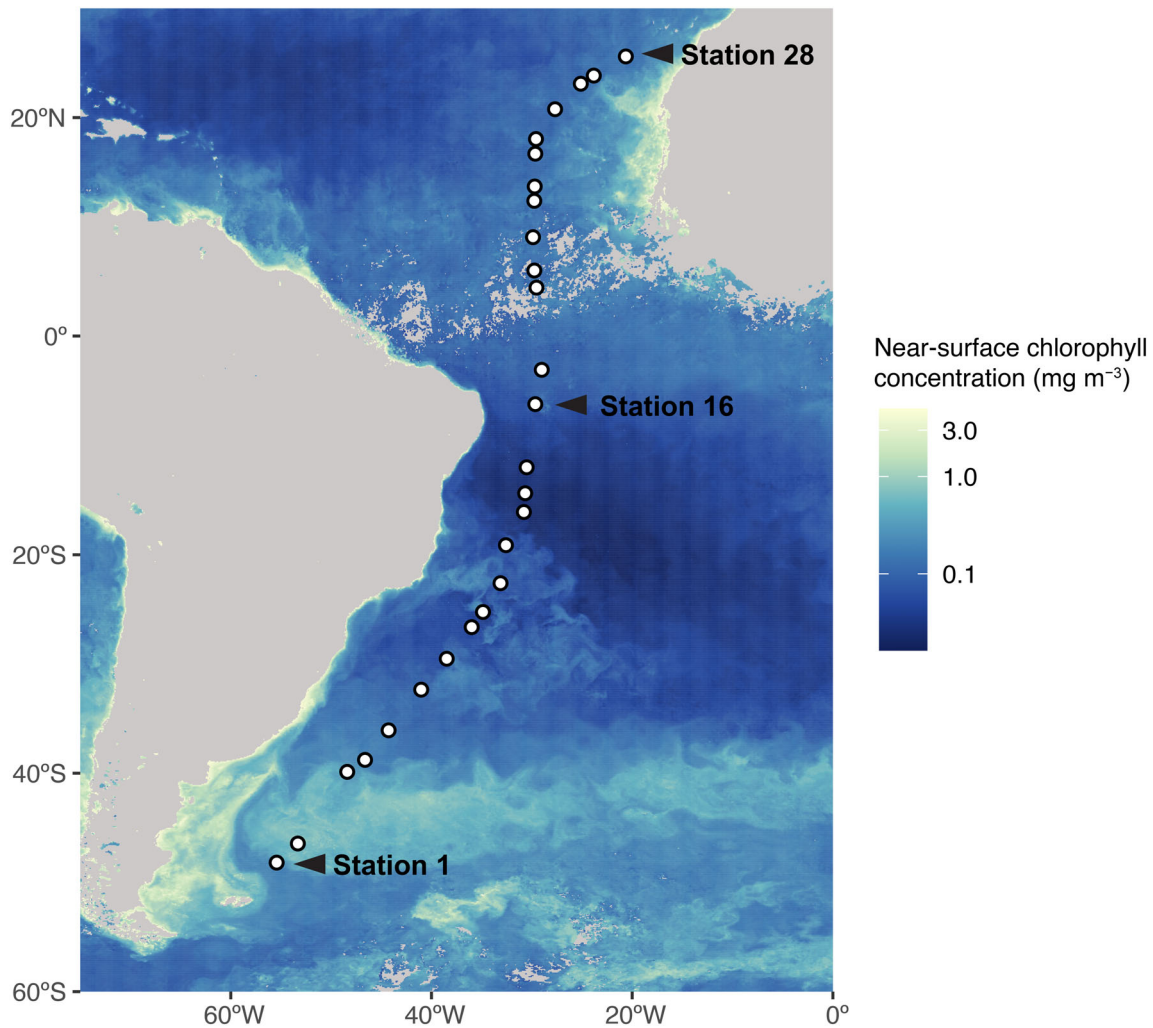


**Fig. 1.** Near-surface chlorophyll concentrations and station positions. Transect of the Poseidon Expedition along the South and Central Atlantic Ocean. Colors represent the near-surface chlorophyll concentration ( $\text{mg m}^{-3}$ ) in March 2019. Data extracted from the Suomi-NPP/Visible Infrared Imaging Radiometer Suite instrument (SNPP-VIIRS) instrument in <https://oceancolor.gsfc.nasa.gov/13/>. Each dot represents one station, numbered from 1 to 28. Note that station 15 does not exist.

Supporting Information Fig. S4). The AAP abundance ranged between undetectable values below the DCM (in 7% of the samples) and  $5.89 \times 10^4$  cells  $\text{mL}^{-1}$  (mean  $\pm$  SD,  $1.19 \times 10^4 \pm 1.11 \times 10^4$  cells  $\text{mL}^{-1}$ ), surpassing the abundances of *Synechococcus* and picoeukaryotes in most samples by an order of magnitude. In some stations within the oligotrophic gyre (stations 11 and 12), with deep DCMs, AAP bacteria cells were detected down to 280 m depth (our deepest sampling). AAP bacteria represented between 0.05% and 8.02% of total bacterioplankton (mean  $\pm$  SD,  $1.47\% \pm 1.11\%$ ). The highest values were observed in the eutrophic southernmost stations and in the equatorial upwelling, corresponding to samples with relatively high concentrations of Chl *a* ( $n = 146$ , Pearson correlation between untransformed AAP abundances and Chl *a*  $R = 0.62$ ,  $p < 0.005$ , Fig. 2b, and between %AAP and Chl *a*,  $n = 146$ ,  $R = 0.42$ ,  $p < 0.005$ ). This correlation was especially strong

and significant in samples from the DCM and below the DCM ( $n = 27$ , Pearson correlations with Chl *a*  $R = 0.69$ ,  $p < 0.005$  and  $n = 58$ ,  $R = 0.82$ ,  $p < 0.005$ , respectively). Interestingly, in station 10, which had a two peak DCM structure, AAP abundance was maximal coinciding with both DCMs (Supporting Information Fig. S5). All in all, the distribution of AAP bacteria along the water column followed the Chl *a* variation, with maximal abundances generally above the DCM and in some cases, at the DCM (stations 4, 5, 6, 12, 16, 18, 20, 27, and 28; Fig. 2b; Supporting Information Fig. S6). This can also be seen by the high correlation between AAP abundances and turbidity (Supporting Information Fig. S6), which is generally high around the DCM. Also, in most stations, the maximum AAP abundances coincided with the maximum abundances of autotrophic picoplankton, especially in the case of *Prochlorococcus* (Supporting Information Fig. S6). In

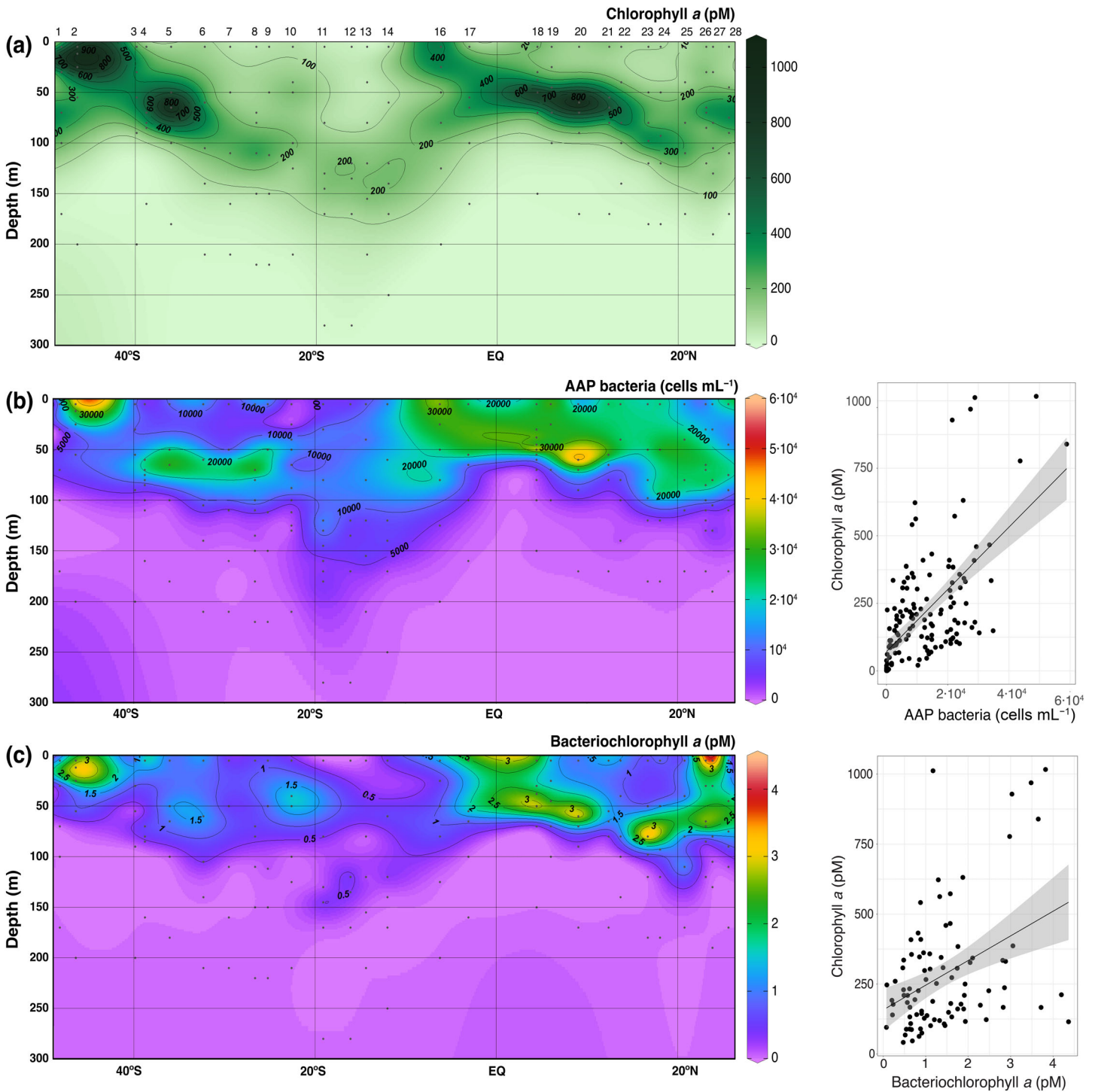


**Fig. 2.** Pigment concentration and abundance of aerobic anoxygenic phototrophic (AAP) bacteria along the South and Central Atlantic Ocean. **(a)** Sectional distribution of chlorophyll *a* (Chl *a*, pM) from the high-performance liquid chromatography (HPLC) analyses. **(b)** Sectional distribution of AAP abundance (cells mL<sup>-1</sup>) estimated by epifluorescence microscopy (left) and its correlation with Chl *a* concentration (right, slope of the linear regression = 0.015,  $p < 0.001$ ). **(c)** Bacteriochlorophyll *a* concentration (pM) estimated with HPLC (left) and its correlation with Chl *a* concentration (right, slope = 109.83,  $p < 0.001$ ). Station numbers are indicated above **(a)** and **(b)**. Black dots in the left panels indicate the sampling depths. The black lines in the correlation plots represent linear regressions and the gray areas represent 95% confidence level interval around the slope estimate.

contrast, in the deepest samples of the dataset, where the concentrations of nitrate, phosphate, and silicate were higher, the abundances of AAP bacteria were near zero in most cases, and in consequence, a negative correlation between nutrients and AAP bacteria abundances was reported (Supporting Information Fig. S6).

### Bacteriochlorophyll *a* distribution

Bacteriochlorophyll *a* concentration in the upper 150 m of the water column varied between 0 and 4.36 pM (mean  $\pm$  SD,  $1.43 \pm 0.98$  pM). The total concentration of Chl *a* was at least two orders of magnitude higher than that of BChl *a* and varied between 0.89 and 1016.45 pM (mean  $\pm$  SD,  $209.07 \pm 205.27$  pM). As shown for AAP abundances, the distribution of BChl *a* was highly correlated with that of Chl *a* ( $n = 147$ , Pearson correlation between BChl *a* and Chl *a*  $R = 0.56$ ,  $p < 0.001$ , Fig. 2c). When we considered only the surface samples, the correlation was weaker ( $n = 27$ , Pearson correlation  $R = 0.41$ ,  $p < 0.05$ ; Supporting Information Fig. S7). In almost all samples, BChl *a* concentration peaked above or at the DCM (Fig. 2), except for a few sites (stations 1, 4, 21, and 27), where BChl *a* was highest at the surface. The variation of BChl *a* also correlated positively with the abundance of autotrophic picoplankton and turbidity, while it had a negative correlation with depth, nitrate, and phosphate (Supporting Information Fig. S6). The proportion of

BChl *a* in total photosynthetic pigments (BChl *a*/[BChl *a* + Chl *a*]), ranged from 0% to 3.65%, being higher in the surface and decreasing in samples from deeper DCM layers (Supporting Information Fig. S8). Finally, the BChl *a* cellular quota ranged between 0.01 and 0.81 fg cell<sup>-1</sup> (mean  $\pm$  SD,  $0.05 \pm 0.09$  fg cell<sup>-1</sup>).

### Light energy captures by AAP bacteria and phytoplankton

The concentration of Chl *a*-containing photosynthetic units (PSUs) varied between  $1.78 \times 10^9$  and  $2.04 \times 10^{12}$  PSU L<sup>-1</sup>, exceeding by around two orders of magnitude BChl *a*-containing PSUs ( $1.34 \times 10^9$  to  $7.73 \times 10^{10}$  PSU L<sup>-1</sup>). Chl *a*-containing PSUs significantly increased from surface toward the DCM and then decreased (Tukey test,  $p < 0.05$ ; Supporting Information Fig. S9), while the concentration of BChl *a* containing PSUs was very similar in the surface, above the DCM or in the DCM (Tukey test,  $p = 0.665$ ), and only significantly decreased below the DCM (Supporting Information Fig. S9, Tukey test,  $p < 0.05$ ), where the pigment concentration was very low. The per-cell light energy captured by each AAP cell ranged between  $3.16 \times 10^{-12}$  and  $2.44 \times 10^{-9}$  J cell<sup>-1</sup> d<sup>-1</sup> (mean  $9.95 \times 10^{-11}$  J cell<sup>-1</sup> d<sup>-1</sup>), about an order of magnitude lower than that utilized by autotrophic picoplankton (mean  $3.76 \times 10^{-10}$  J cell<sup>-1</sup> d<sup>-1</sup>) (Fig. 3a). The cellular light energy captured by autotrophic picoplankton cells increased from the surface to the DCM, consistent with the pattern of increasing

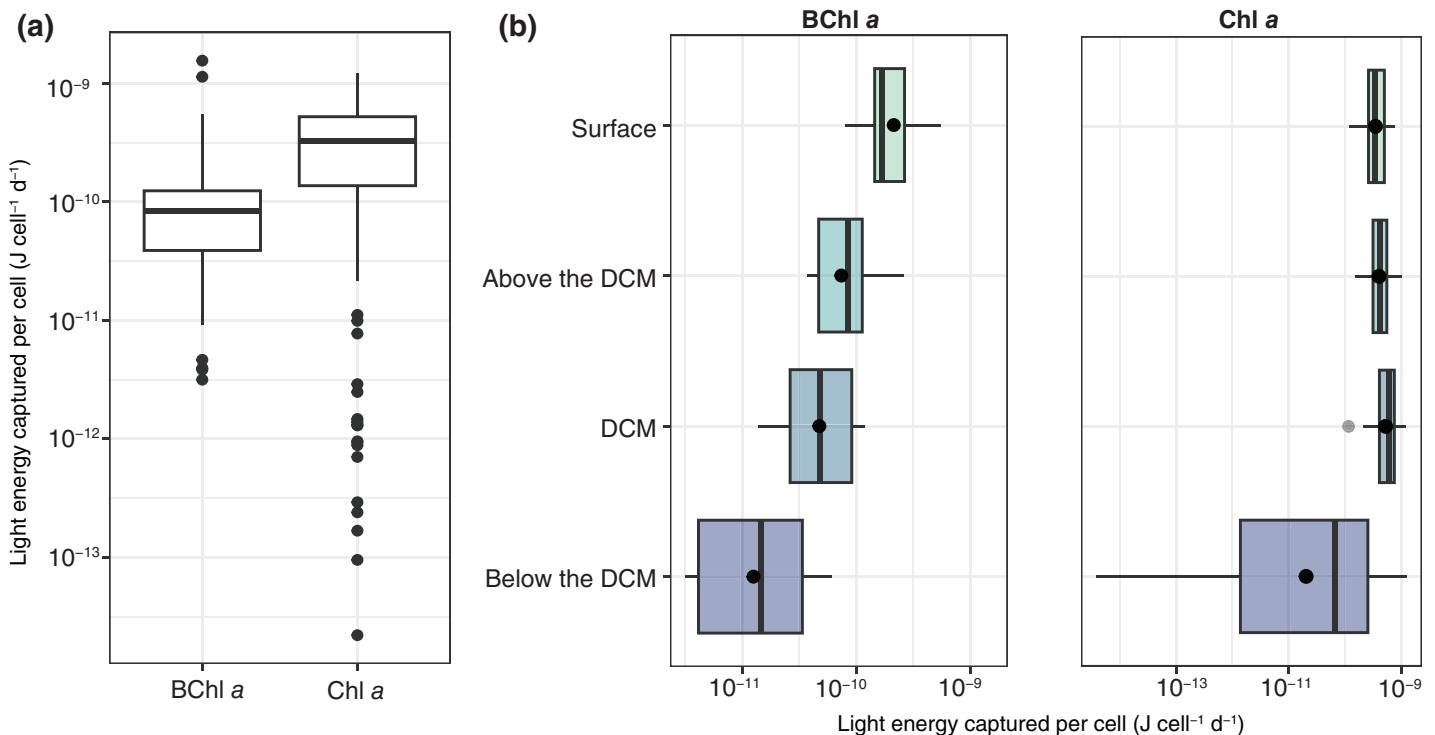


**Fig. 3.** Cellular daily energy captured by bacteriochlorophyll *a* (BChl *a*) and chlorophyll *a* (Chl *a*) along the South and Central Atlantic Ocean. **(a)** Light energy captured per cell and day by BChl *a* and Chl *a*. Outliers are represented with dots outside the boxes. **(b)** Pattern of daily light energy captured per cell by each pigment along the epipelagic layers. The dot within the boxplots is the mean, while the black thick line represents the median.

concentration of Chl *a*-containing PSUs. On the contrary, the light energy harvested by AAP cells significantly decreased with depth (Fig. 3, Tukey test,  $p < 0.005$ ), since while the light intensity declined, the concentration of BChl *a*-containing PSU remained constant across the different epipelagic layers, and was only significantly lower below the DCM. The divergent pattern of energy captured by both pigments along depth becomes evident when representing the ratio of cellular daily energy captured by BChl *a* and Chl *a* in each layer of the epipelagic (Fig. 4a). Aerobic anoxygenic phototrophic bacteria harvest the maximum cellular light energy in the surface, and their contribution rapidly decreases toward deeper waters. At all depths, the values of light energy captured by AAP bacteria exceeds the costs of constructing the proteins and pigments structuring their PSUs (calculated by Kirchman and Hanson (2013) to be ca.  $8.29 \times 10^{-15}$  J per PSU), with a mean net benefit of  $1.47 \times 10^{-10}$  J cell $^{-1}$  d $^{-1}$ . Finally, we estimated the depth-integrated energy potentially captured by AAP bacteria and by autotrophic picoplankton in the water column (Fig. 4b). For both pigments, the concentration of PSU per square meter was higher at more productive regions and lower in the oligotrophic gyres. In contrast to the differences observed between AAP bacteria and the picophytoplankton along the vertical gradient, both groups displayed the same horizontal pattern of estimated energy captured, with lowest values in the South Atlantic oligotrophic gyre, that increased toward more eutrophic sites (Fig. 4b, Pearson correlation of depth-integrated energy captured,  $n = 27$ ,  $R = 0.49$ ,  $p < 0.05$ ).

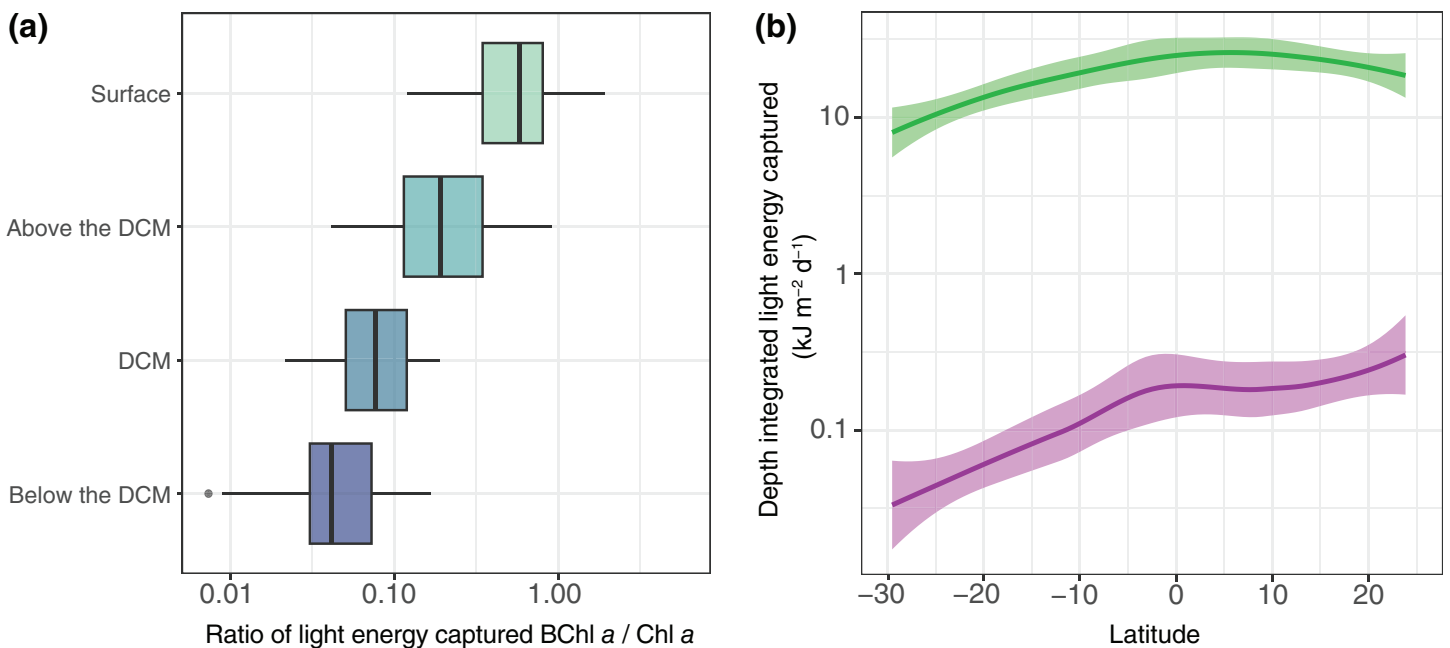


**Fig. 4.** Vertical and horizontal cellular daily energy captured. (a) Ratio of the cellular daily energy captured by bacteriochlorophyll *a* (BChl *a*) and by chlorophyll *a* (Chl *a*) at each layer within the epipelagic, and (b) depth integrated light energy captured by phytoplankton (green line) and aerobic anoxygenic phototrophic (AAP) bacteria (purple line) along the Atlantic Ocean transect.



et al. 2021). Picoeukaryotes also contributed significantly to the total C biomass in the Atlantic Ocean, as seen before by the Atlantic Meridional Transects (Tarran et al. 2006). In our samples, these three groups—*Synechococcus*, *Prochlorococcus*, and picoeukaryotes—were likely the main components of the phytoplankton in most of the transect, with the exception of stations 1–4, where diatoms probably represented an important fraction of the total phytoplankton, as seen by the high values of fucoxanthin in samples from those stations. All in all, the sampled transect showed a high variability in terms of trophic conditions which was reflected in the DCM structures along the water column, with some DCMs being more shallow, while others were located below the 100 m depth.

Along these variable vertical profiles, the abundance of AAP bacteria followed the Chl *a* distribution ( $n = 146$ , Pearson correlation  $R = 0.62$ ,  $p < 0.005$ ; Fig. 2b; Supporting Information Fig. S6), peaking above or at the DCM level, and in most samples coinciding with the autotrophic picoplankton maximum abundances, confirming the outlined hypothesis that AAP bacteria would covary with the DCM structure. Their abundances oscillated around  $10^4$  through the first tens of meters, and decreased from  $10^3$  to zero below 100 m depth. The highest AAP abundances, of around  $4 \times 10^4$  cells  $\text{mL}^{-1}$ , were observed in the eutrophic southernmost stations and in the equatorial upwelling, where the input of nutrients from below the epipelagic zone supports productivity of the phytoplankton communities (Cullen 1982). Likewise, the distribution of both BChl *a* and Chl *a* was very similar ( $n = 147$ ,  $R = 0.59$ ,  $p < 0.001$ ; Fig. 2c; Supporting Information Fig. S6) and these pigments occupied similar areas along the water column. The concentration of BChl *a* in our sampling was comparable to that in other marine regions like the Pacific Ocean (Kolber et al. 2001; Goericke 2002; Lami et al. 2007; Jiao et al. 2010), the Atlantic Ocean (Cottrell et al. 2006; Sieracki et al. 2006), the Baltic Sea (Koblížek et al. 2005), and the Mediterranean Sea (Lami et al. 2009; Hojerová et al. 2011; Ferrera et al. 2014; Gómez-Consarnau et al. 2019), with a mean concentration of 1.43 pM, and surpassing 4.00 pM in some samples.

It has been extensively documented that AAP bacteria are more abundant in more productive areas (reviewed in Koblížek 2015), and the overlap between AAP cells and Chl *a* has been reported before in regions of the Atlantic and Pacific Oceans (Kolber et al. 2001; Schwalbach and Fuhrman 2005; Cottrell et al. 2006; Mašín et al. 2006; Jiao et al. 2007, 2010), and the Mediterranean Sea (Hojerová et al. 2011), yet information along vertical profiles has mainly been obtained from the Northern hemisphere (Mašín et al. 2006; Sieracki et al. 2006; Lami et al. 2009; Hojerová et al. 2011). The AAP abundance values reported in this study are similar to those recorded in oligotrophic waters like the Sargasso Sea (Sieracki et al. 2006; Koblížek et al. 2007) or the North Pacific Gyre (Cottrell et al. 2006; Koblížek et al. 2024), and lower than other more eutrophic areas, while the vertical variation seems to follow a similar trends across different sites (Sieracki et al. 2006; Hojerová et al. 2011).

Environmental variables such as temperature or salinity did not influence the distribution of BChl *a* in our dataset, and the concentration of nutrients like nitrate or phosphate were negatively correlated to both AAP abundances and BChl *a*. This probably reflects the fact that the concentration of these nutrients is high in deeper waters, where the abundance of AAP bacteria is very low. The fact that BChl *a* concentration mirrors the distribution of Chl *a* throughout depth and along the latitudinal axis could indicate that the photoheterotrophic activity of AAP bacteria might be favored or controlled by the same mechanisms that control phytoplankton, but it could also indicate the existence of strong biotic interactions between these two microbial guilds. In fact, co-occurrence networks have shown interactions of some AAP bacteria with the abundance of phototrophic eukaryotes (Auladell et al. 2019), and various AAP species have been isolated from phytoplankton, particularly from dinoflagellate cultures (Biebl et al. 2005; Yang et al. 2018). Interestingly, both pigments had a different correlation with light irradiance. Chlorophyll *a* did not show any correlation with  $\text{PAR}_{(z)}$  ( $R = -0.11$ ,  $p = 0.19$ ), while only BChl *a* concentration had a positive and significant correlation with solar irradiance ( $R = 0.35$ ,  $p < 0.001$ ), probably due to the high values of BChl *a* in the surface of stations 3, 4, 26, or 27 (Fig. 2c), compared to deeper samples. While the bulk BChl *a* concentration changed across depth, along with solar irradiance, the number of BChl *a*-containing PSUs per cell did not statistically vary along the vertical axis (ANOVA,  $p = 0.665$ ), suggesting that no photo-acclimation processes were operating, or at least we could not detect them. The absence of photo-adaptation in AAP populations was also reported when comparing oceanic and estuarine waters, with notable differences in light availability (Cottrell et al. 2010). Although a transcriptional regulator of photosynthesis, *ppsR*, has been described in several AAP bacteria (Lietenberg et al. 2008; Tomasch et al. 2011; Zheng et al. 2011), different species show variable adaptations to changes in light intensity. Culture-based studies revealed that *Roseobacter litoralis* decreased three times the number of BChl *a* molecules in their PSUs (Selyanin et al. 2016), and also *Dinoroseobacter shibae* adjusted its electron transport rate following increasing irradiance (Piwosz et al. 2018). These studies are, however, based on cultivated AAP species and there is little information regarding their phototrophic activity that can be applied to natural communities. Thus, following the approaches used by other authors (Kirchman and Hanson 2013; Gómez-Consarnau et al. 2019), we assumed a constant number of molecules per PSU and a constant electron transfer rate in our calculations.

Previous approaches estimating the light energy captured by AAP bacteria in natural environments were either theoretical (Kirchman and Hanson 2013) or based solely on pigment data and hypothesized AAP abundances (Gómez-Consarnau et al. 2019). Following such studies, we estimated the light energy captured by AAP cells and autotrophic picoplankton, based on in situ cell abundances and pigment concentration

data, and provided, for the first time, a more accurate picture of the potential phototrophy of AAP bacteria in the open ocean. Our data show that photoheterotrophy is especially strong at the surface, where the light energy captured by AAP cells is highest (mean  $4.43 \times 10^{-10}$  J cell<sup>-1</sup> d<sup>-1</sup> in the surface, Fig. 3b) and, in some stations, comparable to that captured by the picophytoplankton (Fig. 4a). All in all, the light energy captured by BChl *a* (mean  $9.95 \times 10^{-11}$  J cell<sup>-1</sup> d<sup>-1</sup>) was about an order of magnitude lower than that captured by Chl *a* (mean  $3.76 \times 10^{-10}$  J cell<sup>-1</sup> d<sup>-1</sup>, Fig. 3a). This additional source of energy gained from light cannot cover the maintenance energy costs of an AAP bacterium cell, estimated to be between  $2 \times 10^{-10}$  and  $4 \times 10^{-10}$  J cell<sup>-1</sup> d<sup>-1</sup> (Kirchman and Hanson 2013), although it probably replaces part of the oxidative phosphorylation, as seen in laboratory experiments (Koblížek et al. 2010; Hauruseu and Koblížek 2012), providing a fraction of the cell metabolic needs and saving substrates that can be further used for biosynthesis (Hauruseu and Koblížek 2012). In fact, it has been estimated that about 20% of AAP cellular energetic requirements could be satisfied by photoheterotrophy (Kolber et al. 2001), indicating a significant reduction in their organic carbon consumption (Jiao et al. 2010). Taken together, these results suggest that AAP photosynthetic activity likely reduces respiration in surface waters, and, in areas where they are abundant, this could have an impact on the global carbon cycle, by reducing their atmospheric CO<sub>2</sub> outputs.

In summary, we show that AAP bacteria are widespread throughout the open ocean in areas of contrasting productivity, from the surface down to 280 m deep. They are strongly associated with the autotrophic picoplankton, as seen by their abundance distribution and BChl *a* variation. The preference of AAP bacteria for chlorophyll-rich waters could be due to common variables affecting the distribution of both functional groups or could also indicate their dependence on the phytoplankton. Aerobic anoxygenic phototrophic cells are larger than average bacteria (Sieracki et al. 2006) and display higher growth rates in different ecological scenarios (Koblížek et al. 2007; Ferrera et al. 2011, 2017). To sustain such a dynamic metabolism, they must rely on large quantities of phytoplankton-derived dissolved organic matter, and therefore they preferably develop in eutrophic marine areas. The light harvesting ability provides AAP bacteria with an additional source of energy that can be used to complement their energetic needs, to cellular motility, or to drive transport of dissolved compounds, especially in the surface ocean.

Overall, this is the first study that uses both in situ cell abundances and pigment data to estimate the potential solar energy captured by AAP bacteria in such an extensive area of the open ocean. The extent of our sampling area facilitated the detection of large-scale patterns, allowing predictions of the potential phototrophic activity of AAP bacteria along the epipelagic, and contributes to a better understanding of the energy fluxes in the ocean and, ultimately, in the global

carbon cycle. Future studies exploring the interaction between AAP bacterial communities and the composition and abundance of organic matter from various phytoplanktonic groups will unveil the intricate relationship between these functional entities. This research will offer insights into the ecological significance of AAP bacteria in marine environments, enhancing our understanding of their pivotal role in ecosystem dynamics.

### Data availability statement

Abundance and pigment data, as well as code for the bioenergetic calculations and statistics is available at [https://github.com/crgazulla/AAP\\_bacteria\\_Atlantic\\_Ocean](https://github.com/crgazulla/AAP_bacteria_Atlantic_Ocean).

### References

- Auladell, A., P. Sánchez, O. Sánchez, J. M. Gasol, and I. Ferrera. 2019. Long-term seasonal and interannual variability of marine aerobic anoxygenic phototrophic bacteria. *ISME J.* **13**: 1975–1987. doi:10.1038/s41396-019-0401-4
- Azam, F., T. Fenchel, J. Field, J. Gray, L. Meyer-Reil, and F. Thingstad. 1983. The ecological role of the water-column microbes in the sea. *Mar. Ecol. Prog. Ser.* **10**: 257–263. doi:10.1021/acs.joc.6b00938
- Béjà, O., and others. 2000. Bacterial rhodopsin: Evidence for a new type of phototrophy in the sea. *Science* **289**: 1902–1906. doi:10.1126/science.289.5486.1902
- Bennke, C. M., G. Reintjes, M. Schattenhofer, A. Ellrott, J. Wulf, M. Zeder, and B. M. Fuchs. 2016. Modification of a high-throughput automatic microbial cell enumeration system for shipboard analyses. *Appl. Environ. Microbiol.* **82**: 3289–3296. doi:10.1128/AEM.03931-15
- Biebl, H., M. Allgaier, B. J. Tindall, M. Koblížek, H. Lünsdorf, R. Pukall, and I. Wagner-Döbler. 2005. *Dinoroseobacter shibae* gen. nov., sp. nov., a new aerobic phototrophic bacterium isolated from dinoflagellates. *Int. J. Syst. Evol. Microbiol.* **55**: 1089–1096. doi:10.1099/ijls.0.63511-0
- Biebl, H., and I. Wagner-Döbler. 2006. Growth and bacteriochlorophyll *a* formation in taxonomically diverse aerobic anoxygenic phototrophic bacteria in chemostat culture: Influence of light regime and starvation. *Process Biochem.* **41**: 2153–2159. doi:10.1016/j.procbio.2006.06.029
- Carvalho, A. C. O., R. Kerr, C. R. B. Mendes, J. L. L. Azevedo, and V. N. Tavano. 2021. Phytoplankton strengthen CO<sub>2</sub> uptake in the South Atlantic Ocean. *Prog. Oceanogr.* **190**: 102476. doi:10.1016/j.pocean.2020.102476
- Cottrell, M. T., A. Mannino, and D. L. Kirchman. 2006. Aerobic anoxygenic phototrophic bacteria in the Mid-Atlantic Bight and the North Pacific gyre. *Appl. Environ. Microbiol.* **72**: 557–564. doi:10.1128/AEM.72.1.557-564.2006
- Cottrell, M. T., J. Ras, and D. L. Kirchman. 2010. Bacteriochlorophyll and community structure of aerobic anoxygenic

- phototrophic bacteria in a particle-rich estuary. *ISME J.* **4**: 945–954. doi:[10.1038/ismej.2010.13](https://doi.org/10.1038/ismej.2010.13)
- Cullen, J. J. 1982. The deep chlorophyll maximum: Comparing vertical profiles of chlorophyll *a*. *Can. J. Fish. Aquat. Sci.* **39**: 791–803.
- Fecskeová, L. K., K. Piwosz K, D. Šantić, S. Šestanović, A. V. Tomaš, M. Hanusová, M. Šolić, and M. Koblížek. 2021. Lineage-specific growth curves document large differences in response of individual groups of marine bacteria to the top-down and bottom-up controls. *mSystems* **6**: e00934-21. doi:[10.1128/mSystems.00934-21](https://doi.org/10.1128/mSystems.00934-21)
- Ferrera, I., J. M. Gasol, M. Sebastián, E. Hojerová, and M. Koblížek. 2011. Comparison of growth rates of aerobic anoxygenic phototrophic bacteria and other bacterioplankton groups in coastal Mediterranean waters. *Appl. Environ. Microbiol.* **77**: 7451–7458. doi:[10.1128/AEM.00208-11](https://doi.org/10.1128/AEM.00208-11)
- Ferrera, I., C. M. Borrego, G. Salazar, and J. M. Gasol. 2014. Marked seasonality of aerobic anoxygenic phototrophic bacteria in the coastal NW Mediterranean Sea as revealed by cell abundance, pigment concentration and pyrosequencing of *pufM* gene. *Environ. Microbiol.* **16**: 2953–2965. doi:[10.1111/1462-2920.12278](https://doi.org/10.1111/1462-2920.12278)
- Ferrera, I., O. Sánchez, E. Kolářová, M. Koblížek, and J. M. Gasol. 2017. Light enhances the growth rates of natural populations of aerobic anoxygenic phototrophic bacteria. *ISME J.* **11**: 2391–2393. doi:[10.1038/ismej.2017.79](https://doi.org/10.1038/ismej.2017.79)
- Gasol, J. M., and X. A. G. Morán. 2015. Flow cytometric determination of microbial abundances and its use to obtain indices of community structure and relative activity. In T. J. McGenity, K. N. Timmis, and B. Nogales [eds.], *Hydrocarbon and lipid microbiology protocols*. Springer protocols handbooks. Springer. doi:[10.1007/8623\\_2015\\_139](https://doi.org/10.1007/8623_2015_139)
- Gazulla, C. R. 2024. Ecology of marine aerobic anoxygenic phototrophic bacteria. Ph.D. Thesis. Univ. Autònoma de Barcelona.
- Gazulla, C. R., A. Auladell, C. Ruiz-González, P. C. Junger, C. M. Duarte, J. M. Gasol, O. Sánchez, and I. Ferrera. 2022. Global diversity and distribution of aerobic anoxygenic phototrophs in the tropical and subtropical oceans. *Environ. Microbiol.* **24**: 2222–2238. doi:[10.1111/1462-2920.15835](https://doi.org/10.1111/1462-2920.15835)
- Goericke, R. 2002. Bacteriochlorophyll *a* in the ocean: Is anoxygenic bacterial photosynthesis important? *Limnol. Oceanogr.* **47**: 290–295. doi:[10.4319/lo.2002.47.1.0290](https://doi.org/10.4319/lo.2002.47.1.0290)
- Goericke, R., and D. J. Repeta. 1993. Chlorophylls *a* and *b* and divinyl chlorophylls *a* and *b* in the open subtropical North Atlantic Ocean. *Mar. Ecol. Prog. Ser.* **101**: 307–313.
- Gómez-Consarnau, L., and others. 2019. Microbial rhodopsins are major contributors to the solar energy captured in the sea. *Sci. Adv.* **5**: 1–8. doi:[10.1126/sciadv.aaw8855](https://doi.org/10.1126/sciadv.aaw8855)
- González-Vega, A., J. M. Arrieta, M. Santana-Casiano, M. González-Dávila, C. Santana-González, J. M. Mercado, J. Escáñez-Pérez, C. Presas-Navarro, and E. Fraile-Nuez. 2023. Tagoro submarine volcano as a natural source of significant dissolved inorganic nutrients. In P. J. González [ed.], *El Hierro Island. Active volcanoes of the world*. Springer. doi:[10.1007/978-3-031-35135-8\\_9](https://doi.org/10.1007/978-3-031-35135-8_9)
- Harashima, K., M. Nakagawa, and N. Murata. 1982. Photochemical activities of bacteriochlorophyll in aerobically grown cells of aerobic heterotrophs, *Erythrobacter* species (OCh 114) and *Erythrobacter longus* (OCh 101). *Plant Cell Physiol.* **23**: 185–193. doi:[10.1093/oxfordjournals.pcp.a076338](https://doi.org/10.1093/oxfordjournals.pcp.a076338)
- Harrell, F. E. 2024. Hmisc: Harrell miscellaneous. R package version 5.1-2. Available from <https://hbiostat.org/R/Hmisc/>
- Hartmann, M., C. Grob, G. A. Tarran, A. Martin, P. Burkill, D. Scanlan, and M. V. Zubkov. 2012. Mixotrophic basis of Atlantic oligotrophic ecosystems. *Proc. Natl. Acad. Sci. USA* **109**: S756–S760. doi:[10.1073/pnas.1118179109](https://doi.org/10.1073/pnas.1118179109)
- Hauruseu, D., and M. Koblížek. 2012. Influence of light on carbon utilization in aerobic anoxygenic phototrophs. *Appl. Environ. Microbiol.* **78**: 7414–7419. doi:[10.1128/AEM.01747-12](https://doi.org/10.1128/AEM.01747-12)
- Hojerová, E., M. Mašín, C. Brunet, I. Ferrera, J. M. Gasol, and M. Koblížek. 2011. Distribution and growth of aerobic anoxygenic phototrophs in the Mediterranean Sea. *Environ. Microbiol.* **13**: 2717–2725. doi:[10.1111/j.1462-2920.2011.02540.x](https://doi.org/10.1111/j.1462-2920.2011.02540.x)
- Imhoff, J. F. 2017. Diversity of anaerobic anoxygenic phototrophic purple bacteria. In P. Hallenbeck [ed.], *Modern topics in the phototrophic prokaryotes*. Springer. doi:[10.1007/978-3-319-46261-5\\_2](https://doi.org/10.1007/978-3-319-46261-5_2)
- Jiao, N., F. Zhang, and N. Hong. 2010. Significant roles of bacteriochlorophyll *a* supplemental to chlorophyll *a* in the ocean. *ISME J.* **4**: 595–597. doi:[10.1038/ismej.2009.135](https://doi.org/10.1038/ismej.2009.135)
- Jiao, N., Y. Zhang, Y. Zeng, N. Hong, R. Liu, F. Chen, and P. Wang. 2007. Distinct distribution pattern of abundance and diversity of aerobic anoxygenic phototrophic bacteria in the global ocean. *Environ. Microbiol.* **9**: 3091–3099. doi:[10.1111/j.1462-2920.2007.01419.x](https://doi.org/10.1111/j.1462-2920.2007.01419.x)
- Kirchman, D. L., and T. E. Hanson. 2013. Bioenergetics of photoheterotrophic bacteria in the oceans. *Environ. Microbiol. Rep.* **5**: 188–199. doi:[10.1111/j.1758-2229.2012.00367.x](https://doi.org/10.1111/j.1758-2229.2012.00367.x)
- Koblížek, M. 2015. Ecology of aerobic anoxygenic phototrophs in aquatic environments. *FEMS Microbiol. Rev.* **39**: 854–870. doi:[10.1093/femsre/fuv032](https://doi.org/10.1093/femsre/fuv032)
- Koblížek, M., J. Stoń-Egiert, S. Sagan, and Z. S. Kolber. 2005. Diel changes in bacteriochlorophyll *a* concentration suggest rapid bacterioplankton cycling in the Baltic Sea. *FEMS Microbiol. Ecol.* **51**: 353–361. doi:[10.1016/j.femsec.2004.09.016](https://doi.org/10.1016/j.femsec.2004.09.016)
- Koblížek, M., M. Mašín, J. Ras, A. J. Poulton, and O. Prasil. 2007. Rapid growth rates of aerobic anoxygenic phototrophs in the ocean. *Environ. Microbiol.* **9**: 2401–2406. doi:[10.1111/j.1462-2920.2007.01354.x](https://doi.org/10.1111/j.1462-2920.2007.01354.x)
- Koblížek, M., J. Mlčoušková, Z. S. Kolber, and J. Kopecký. 2010. On the photosynthetic properties of marine

- bacterium COL2P belonging to *Roseobacter* clade. Arch. Microbiol. **192**: 41–49. doi:10.1007/s00203-009-0529-0
- Koblížek, M., I. Ferrera, E. Kolářová, S. Duhamel, K. J. Popendorf, J. M. Gasol, and B. A. S. Van Mooy. 2024. Growth and mortality of aerobic anoxygenic phototrophs in the North Pacific Subtropical Gyre. Appl. Environ. Microbiol. **90**: e00032-24. doi:10.1128/aem.00032-24
- Kolber, Z. S., C. L. Van Dover, R. A. Niederman, and P. G. Falkowski. 2000. Bacterial photosynthesis in surface waters of the open ocean. Nature **407**: 177–179. doi:10.1038/35025044
- Kolber, Z. S., and others. 2001. Contribution of aerobic photoheterotrophic bacteria to the carbon cycle in the ocean. Science **292**: 2492–2495. doi:10.1126/science.1059707
- Lami, R., M. T. Cottrell, J. Ras, O. Ulloa, I. Obernosterer, H. Claustre, D. L. Kirchman, and P. Lebaron. 2007. High abundances of aerobic anoxygenic photosynthetic bacteria in the South Pacific Ocean. Appl. Environ. Microbiol. **73**: 4198–4205. doi:10.1128/AEM.02652-06
- Lami, R., Z. Čuperová, J. Ras, P. Lebaron, and M. Koblížek. 2009. Distribution of free-living and particle-attached aerobic anoxygenic phototrophic bacteria in marine environments. Aquat. Microb. Ecol. **55**: 31–38. doi:10.3354/ame01282
- Lamy, D., and others. 2011. Seasonal dynamics of aerobic anoxygenic phototrophs in a Mediterranean coastal lagoon. Aquat. Microb. Ecol. **62**: 153–163. doi:10.3354/ame01467
- Liotenberg, S., A.-S. Steunou, M. Picaud, F. Reiss-Husson, C. Astier, and S. Ouchane. 2008. Organization and expression of photosynthesis genes and operons in anoxygenic photosynthetic proteobacteria. Environ. Microbiol. **10**: 2267–2276. doi:10.1111/j.1462-2920.2008.01649.x
- Madigan, M. T., and D. O. Jung. 2009. An overview of purple bacteria: Systematics, physiology, and habitats. In C. N. Hunter, F. Daldal, M. C. Thurnauer, and J. T. Beatty [eds.], The purple phototrophic bacteria. Advances in photosynthesis and respiration, v. **28**. Springer. doi:10.1007/978-1-4020-8815-5\_1
- Malviya, S., and others. 2016. Insights into global diatom distribution and diversity in the world's ocean. Proc. Natl. Acad. Sci. USA **113**: E1516–E1525. doi:10.1073/pnas.1509523113
- Mašín, M., A. J. Zdun, M. Stoň-Egiert, M. Nausch, M. Labrenz, V. Moulisová, and M. Koblížek. 2006. Seasonal changes and diversity of aerobic anoxygenic phototrophs in the Baltic Sea. Aquat. Microb. Ecol. **45**: 247–254. doi:10.3354/ame045247
- Piwosz, K., D. Kaftan, J. Dean, J. Šetlík, and M. Koblížek. 2018. Nonlinear effect of irradiance on photoheterotrophic activity and growth of the aerobic anoxygenic phototrophic bacterium *Dinoroseobacter shibae*. Environ. Microbiol. **20**: 724–733. doi:10.1111/1462-2920.14003
- Piwosz, K., C. Villena-Aleman, and I. Mujakić. 2022. Photoheterotrophy by aerobic anoxygenic bacteria modulates carbon fluxes in a freshwater lake. ISME J. **16**: 1046–1054. doi:10.1038/s41396-021-01142-2
- Rathgeber, C., and others. 2008. Vertical distribution of the aerobic phototrophic bacteria at the Juan de Fuca Ridge in the Pacific Ocean. Photosynth. Res. **97**: 235–244. doi:10.1007/s11120-008-9332-z
- R Core Team 2024. R: A Language and Environment for Statistical Computing. R Foundation for Statistical Computing. Vienna, Austria. Available from <https://www.R-project.org>
- Ritchie, A. E., and Z. I. Johnson. 2012. Abundance and genetic diversity of aerobic anoxygenic phototrophic bacteria of coastal regions of the Pacific Ocean. Appl. Environ. Microbiol. **78**: 2858–2866. doi:10.1128/AEM.06268-11
- Sánchez, O., M. Koblížek, J. M. Gasol, and I. Ferrera. 2017. Effects of grazing, phosphorus and light on the growth rates of major bacterioplankton taxa in the coastal NW Mediterranean. Environ. Microbiol. Rep. **9**: 300–309. doi:10.1111/1758-2229.12535
- Sánchez, O., and others. 2020. Seasonal impact of grazing, viral mortality, resource availability and light on the group-specific growth rates of coastal Mediterranean bacterioplankton. Sci. Rep. **10**: 19773. doi:10.1038/s41598-020-76590-5
- Schwalbach, M. S., and J. A. Fuhrman. 2005. Wide-ranging abundances of aerobic anoxygenic phototrophic bacteria in the world ocean revealed by epifluorescence microscopy and quantitative PCR. Limnol. Oceanogr. **50**: 620–628. doi:10.4319/lo.2005.50.2.0620
- Selyanin, V., D. Hauruseu, and M. Koblížek. 2016. The variability of light-harvesting complexes in aerobic anoxygenic phototrophs. Photosynth. Res. **128**: 35–43. doi:10.1007/s11120-015-0197-7
- Sieracki, M. E., I. C. Gilg, E. C. Thier, N. J. Poulton, and R. Goericke. 2006. Distribution of planktonic aerobic anoxygenic photoheterotrophic bacteria in the northwest Atlantic. Limnol. Oceanogr. **51**: 38–46. doi:10.4319/lo.2006.51.1.0038
- Tarran, G. A., J. L. Heywood, and M. V. Zubkov. 2006. Latitudinal changes in the standing stocks of nano- and picoeukaryotic phytoplankton in the Atlantic Ocean. Deep-Sea Res. II Top. Stud. Oceanogr. **53**: 151–1529. doi:10.1016/j.dsr2.2006.05.004
- Tomasch, J., R. Gohl, B. Bunk, M. S. Diez, and I. Wagner-Döbler. 2011. Transcriptional response of the photoheterotrophic marine bacterium *Dinoroseobacter shibae* to changing light regimes. ISME J. **5**: 1957–1968. doi:10.1038/ismej.2011.68
- Visintini, N., A. C. Martiny, and P. Flombaum. 2021. *Prochlorococcus*, *Synechococcus*, and picoeukaryotic phytoplankton abundances in the global ocean. Limnol. Oceanogr. Lett. **6**: 207–215. doi:10.1002/lo2.10188
- Vrdoljak, T. A., D. Šantić, M. Šolić, M. Ordulj, S. Jozić, S. Šestanović, F. Matic, G. Kušpilić, and Z. N. Gladan. 2019. Dynamics of aerobic anoxygenic phototrophs along the trophic gradient in the central Adriatic Sea. Deep-Sea Res. II Top. Stud. Oceanogr. **164**: 112–121. doi:10.1016/j.dsr2.2019.06.001
- Wickham, H. 2016. Elegant graphics for data analysis: ggplot2. Available from <https://ggplot2.tidyverse.org>



- Wickham, H., and others. 2019. Welcome to the Tidyverse. *J. Open. Sour. Softw.* **4**: 1686. doi:10.21105/joss.01686
- Yang, Q., and others. 2018. *Hoeflea prorocentri* sp. nov., isolated from a culture of the marine dinoflagellate *Prorocentrum mexicanum* PM01. *Antonie Van Leeuwenhoek* **111**: 1845–1853. doi:10.1007/s10482-018-1074-0
- Yurkov, V., and H. van Gernerden. 1993. Impact of light/dark regime on growth rate, biomass formation and bacteriochlorophyll synthesis in *Erythromicrobium hydrolyticum*. *Arch. Microbiol.* **159**: 84–89. doi:10.1007/BF00244268
- Yurkov, V. V., and J. T. Beatty. 1998. Aerobic anoxygenic phototrophic bacteria. *Microb. Mol. Biol. Rev.* **62**: 695–724. doi:10.1128/MMBR.62.3.695-724.1998
- Zheng, Q., R. Zhang, M. Koblížek, E. N. Boldareva, V. Yurkov, S. Yan, and N. Jiao. 2011. Diverse arrangement of photosynthetic gene clusters in aerobic anoxygenic phototrophic bacteria. *PLoS One* **6**: 1–7. doi:10.1371/journal.pone.0025050
- Zubkov, M. V., M. A. Sleight, G. A. Tarran, P. H. Burkill, and R. J. G. Leakey. 1998. Picoplankton community structure on an Atlantic transect from 50°N to 50°S. *Deep-Sea Res. II Oceanogr. Res. Pap.* **45**: 1339–1355. doi:10.1016/S0967-0637(98)00015-6
- Zubkov, M. V., M. A. Sleight, P. H. Burkill, and R. J. G. Leakey. 2000. Picoplankton community structure on the Atlantic Meridional Transect: A comparison between seasons. *Prog. Oceanogr.* **45**: 369–386. doi:10.1016/S0079-6611(00)00008-2
- Zubkov, M. V., and G. A. Tarran. 2005. Amino acid uptake of *Prochlorococcus* spp. in surface waters across the South Atlantic Subtropical Front. *Aquat. Microb. Ecol.* **40**: 241–249. doi:10.3354/ame040241

## Acknowledgments

We thank the people of the Laboratory of Anoxygenic Phototrophs in Třeboň, Czech Republic, where the epifluorescence microscopy and HPLC analyses were performed. We are particularly grateful to Lucija Kanjer for her help during optimization of our HPLC protocol. We also thank Dr. Martí Galí (ICM-CSIC) for his help in obtaining the satellite data and Dr. Laura Gómez-Consarnau (University of Southern California) for her guidance in the bioenergetic calculations. We would also like to thank all the crew members of the *R/V Sarmiento de Gamboa*, as well as the POSEIDON Expedition scientific team, particularly Dr. Carolina Marin-Vindas, Dr. Alba González-Vega, Dr. Eugenio Fraile-Nuez, and chief scientist Dr. Jesús M. Arrieta. The authors also thank the two anonymous reviewers that provided valuable comments and helped to improve the manuscript. This work was supported by grants ECLIPSE (PID2019-110128RB-I00/AEI/10.13039/501100011033) to IF and MICOLOR to JMG (PID2021-125469NB-C31/AEI/10.13039/501100011033/FEDER, UE) and OS (PID2021-125469NB-C32/AEI/10.13039/501100011033/FEDER, UE), all funded by the Agencia Estatal de Investigación from the Spanish Ministry of Science and Innovation. Acknowledgement to the “Severo Ochoa Centre of Excellence” accreditation grant (CEX2019-000928-S funded by AEI 10.13039/501100011033). CRG was supported by a PIF fellowship from the Universitat Autònoma de Barcelona. MK was supported by the Photomachines OP JAK project (CZ.02.01.01/00/22\_008/0004624) financed by the Czech Ministry of Education, Youth and Sports. We acknowledge support of the publication fee by the CSIC Open Access Publication Support Initiative through its Unit of Information Resources for Research.

## Conflict of Interest

None declared.

Submitted 03 November 2023

Revised 03 May 2024

Accepted 23 August 2024

Associate Editor: Katherina Petrou